Projectile-breakup-induced fission-fragment angular distributions in the ^{6}Li + ^{232}Th reaction

A. Pal,[1,2,*] S. Santra,[1,2] D. Chattopadhyay,[1,2] A. Kundu,[1,2] K. Ramachandran,[1] R. Tripathi,[2,3] B. J. Roy,[1,2] T. N. Nag,[3] Y. Sawant,[1] D. Sarkar,[1] B. K. Nayak,[1,2] A. Saxena,[1,2] and S. Kailas[1]

[1]*Nuclear Physics Division, Bhabha Atomic Research Centre, Mumbai 400085, India*

[2]*Homi Bhabha National Institute, Anushaktinagar, Mumbai 400094, India*

[3]*Radiochemistry Division, Bhabha Atomic Research Centre, Mumbai 400085, India*

(Received 19 January 2017; revised manuscript received 14 June 2017; published 1 August 2017)

Background: Experimental anisotropy in fission-fragment (FF) angular distribution in reactions involving weakly bound stable projectiles with actinide targets are enhanced compared to statistical saddle-point model (SSPM) predictions. Contributions from breakup- or transfer-induced fission to total fission are cited as possible reasons for such enhancement.

Purpose: To identify the breakup- or transfer-induced fission channels in ^{6}Li+^{232}Th reaction and to investigate their effects on FF angular anisotropy.

Methods: The FF angular distributions have been measured exclusively at three beam energies (28, 32, and 36 MeV) around the Coulomb barrier in coincidence with projectile breakup fragments like α, d, and p using Si strip detectors. The angular anisotropy obtained for different exclusive breakup- or transfer-induced fission channels are compared with that for total fission. SSPM and pre-equilibrium fission models have been employed to obtain theoretical FF angular anisotropy.

Results: Angular anisotropy of the fission fragments produced by different transfer- or breakup-induced fission reactions have been obtained separately in the rest frame of respective recoiling nuclei. Some of these anisotropies were found to be stronger than those of the inclusive fission. Overall angular distributions of transfer or breakup fission, integrated over all possible recoil angles with weight factor proportional to differential cross section of the complementary breakup fragment emitted in coincidence in all possible directions, were obtained. It was observed that the overall FF angular anisotropy for each of these fission channels is less than or equal to the anisotropy of total fission at all the measured energies. Assuming isotropic out-of-plane correlations between the fission fragments and light-charged particles, the overall breakup- or transfer-induced fission fragment angular distributions do not explain the observed enhancement in FF anisotropy of total fission. Pre-equilibrium fission model provides a reasonable explanation of the enhanced experimental anisotropy of total fission.

Conclusions: Angular anisotropies for different breakup or transfer fission channels involving emission of α, d, and p in the reaction plane have been measured for the ^{6}Li + ^{232}Th reaction. The overall FF angular anisotropies of breakup- or transfer-induced fissions do not explain the enhanced anisotropy of total fission at near-barrier energies. A measurement of out-of-plane correlation is necessary to confirm the above observation and obtain a complete picture on the effect of transfer or breakup on total fission.

DOI: 10.1103/PhysRevC.96.024603

I. INTRODUCTION

The study of nuclear reactions involving weakly bound stable projectiles has been very interesting due to the observation of many unconventional features compared to the reactions involving tightly bound projectiles. Fusion suppression at above-barrier energies [1–6], absence of threshold anomaly in the optical model potential for elastic scattering angular distributions [7–10], and large α-particle production [11–14] are some of the interesting observations associated with these reactions. Fission-fragment (FF) mass and angular distributions are the other important observables in the reactions involving weakly bound projectiles with actinide targets where several interesting results have been observed [15–18]. For fission reactions involving ^{6}Li as a projectile, a sharp energy dependence in the shape of the FF mass distribution, particulary, the ratio of peak to valley (P/V) of the mass distribution has been observed at below-barrier energies [16,18]. The P/V ratio of the mass distribution is a measure of the compound nucleus temperature. As the value of the P/V ratio is greater, the excitation energy of the compound nucleus is less. The sharp increase in the P/V ratio with the decrease in the beam energy has been concluded to be due to the contribution of incomplete fusion (ICF) followed by fission along with the complete fusion (CF) fission. For ICF, i.e., capture of one of the projectile breakup fragments, only a partial energy gets transferred to the composite nuclei, leading to smaller excitation energies. Hence, breakup of ^{6}Li (^{7}Li) into α and $d(t)$, followed by capture of one of the fragments by the target, leading to fission, is the prime reason for the modification of the overall mass distribution. Second, for ICF fission, the FF folding angles have been observed to increase due to partial linear momentum transfer to the target at above-barrier energies with grazing angle $\theta_{gr} < 90^{\circ}$, whereas at below-barrier energies with $\theta_{gr} > 90^{\circ}$ the FF folding angle decreases due to higher linear momentum transfer compared to complete-fusion fission. So the presence of projectile breakup is responsible for populating the composite nuclei with different temperature and recoil energy, leading to such unusual features in fission observables.

*asimpal@barc.gov.in

Fission-fragment angular distribution is another important observable where the projectile breakup may play a dynamic role in modifying the angular anisotropy. The FF angular distributions for CF fission and transfer- or breakup-induced fission are expected to be different as the temperature and the angular momentum in the fissioning nuclei are different in these two processes. In the study of transfer-induced fission in the ^{16}O + ^{232}Th system [19], Lestone *et al.* have observed a strong fission-fragment angular correlation with respect to the recoil direction of the fissioning nuclei. However, integration over all recoil angles results in a weak distribution relative to the beam direction. From the folding angle distributions of the fission fragments, Kailas *et al.* [20] have been able to separate the transfer-induced fission and compound nucleus fission for ^{11}B + ^{237}Np, ^{12}C + ^{236}U, and ^{16}O + ^{232}Th systems. They concluded that at energies close to the Coulomb barrier, the transfer fission component is not significant enough to modify the anisotropy values obtained from the total FF angular distribution. Using the same technique, Majumdar *et al.* [21] and Hinde *et al.* [22] have separated out the fission events following full momentum transfer for ^{19}F + ^{232}Th and ^{16}O + ^{238}U system respectively. Angular anisotropy values for CF-fission events were observed to be more compared to inclusive fission events at sub-barrier energies. Zhang *et al.* [23] observed anomalous increase in anisotropy at sub-barrier energy for ^{19}F + ^{232}Th system and considered transfer-induced fission as one of the possible reasons; however, they found that the contribution of transfer-induced fission is not so significant (∼10%). But in case of a reaction involving ^{6}Li or ^{7}Li as projectile, due to their low breakup threshold, the contribution of tranfer- or breakup-induced fission could be significant as a direct manifestation of large suppression (∼25–30%) of complete fusion [1,5,6].

In our earlier measurement for ^{6,7}Li + ^{235,238}U systems [17], the FF angular anisotropies have been observed to be higher than the ones expected from SSPM predictions. It has been concluded that the observed discrepancy may be due to the combined effect of entrance-channel-dependent pre-equilibrium fission and transfer- or breakup-induced fission. At near-barrier energies, for lower ground-state spin, the entrance channel K (projection of J along the nuclear symmetry axis) distribution becomes narrower, leading to an enhanced anisotropy compared to the SSPM prediction. On the other hand, a significant contribution from α- and d/t-induced fission with different K_0^2 and $\langle J^2 \rangle$ may be responsible for the anomalous anisotropy of total fission. Similar conclusions can also be made on the existing data on FF angular distributions for ^{6,7}Li + ^{232}Th systems measured by Freiesleben *et al.* [15]. However, there is no data available in the literature on the individual transfer- or breakup-induced fission channels and their contributions responsible for overall angular anisotropy of the total fission fragments for the above systems. To identify these ICF fission channels and disentangle their individual contributions on total fission, exclusive measurements of fission fragments in coincidence with the complementary breakup fragments or light charged particles are essential.

To get a complete picture of the overall anisotropy due to transfer-induced fission, both the in-plane and out-of-plane anisotropies are necessary in principle. However, contradictory observations on the out-of-plane anisotropy have been reported for different systems [19,24,25]. While Dyer *et al.* [24] have observed a strong out-of-plane correlation compared to in-plane correlation for the system ^{86}Kr + ^{209}Bi, Lestone *et al.* [19] have observed nearly isotropic (anisotropy ∼0.8–1.1) out-of-plane correlation for ^{16}O + ^{232}Th system. Similarly, Wolf *et al.* [25] have also observed a smaller value for the out-of-plane anisotropy (∼1–1.5) compared to the in-plane anisotropy (∼1.5–2) with respect to the angle of emission of PLF for ^{239}Pu(d, pf) reaction. In particular, when the PLFs are emitted in the backward angles, a nearly isotropic out-of-plane correlation has been observed for both ^{16}O + ^{232}Th as well as d + ^{239}Pu reactions. So, for beam energies near and below the Coulomb barrier, the probability of PLF emission in backward directions (grazing angles) being maximum, the out-of-plane correlation may be expected to be isotropic.

In the present work, the in-plane angular anisotropy for transfer- or breakup-induced fission for the ^{6}Li + ^{232}Th system has been measured exclusively at few energies around the Coulomb barrier to identify the possible transfer or breakup reaction channels leading to fission and to investigate the effect of these ICF fission processes on the total fission fragment angular anisotropy. The detector setup used for the present experiment allowed us to obtain the anisotropy only in the reaction plane.

The paper has been organized in the following way. Experimental details and data analysis methods have been described in Sec. II. The FF angular distributions for total (inclusive) fission measured in the present work and their comparison with existing data as well as SSPM predictions have been described in Sec. III. The angular distributions of transfer or breakup fission in the rest frame of recoil nuclei have been described in Sec. IV. The differential cross sections for the outgoing α, d, and p, and the effect of these ICF channels on the total FF angular anisotropy with respect to beam direction have been discussed in Sec. V. The effect of pre-equilibrium fission has been discussed in Sec. VI. Finally, the results are summarized in Sec. VII.

II. EXPERIMENT AND DATA ANALYSIS

The experiment was carried out using the ^{6}Li beam from BARC-TIFR Pelletron accelerator facility, Mumbai, at three bombarding energies of 28, 32, and 36 MeV. A self-supporting ^{232}Th foil of thickness ∼400 μg/cm^2 was used as a target. A schematic diagram of the experimental setup has been shown in Fig. 1. To detect the fission fragments, four silicon strip detectors, F_1–F_4, of size 50 mm × 50 mm each, covering a total angular range of ∼94–172°, were placed on a fixed arm. Each of these detectors has 16 vertical strips of length 50 mm, breadth 3 mm, and thickness 50 μm. The thickness of the detector is such that only a partial energy of elastically scattered ^{6}Li is deposited but it is sufficiently thick to stop all the fission fragments. The distance of the central strips of each detector from the target center was 176 mm. The gap between two adjacent fission detectors is ∼4°. A typical fission spectrum measured in coincidence with light charged particles by a single strip detector at $E_{\rm beam}$ = 36 MeV is shown in Fig. 2(a). It provides a good separation between light charged particles and fission fragments. A vertical dashed line has been

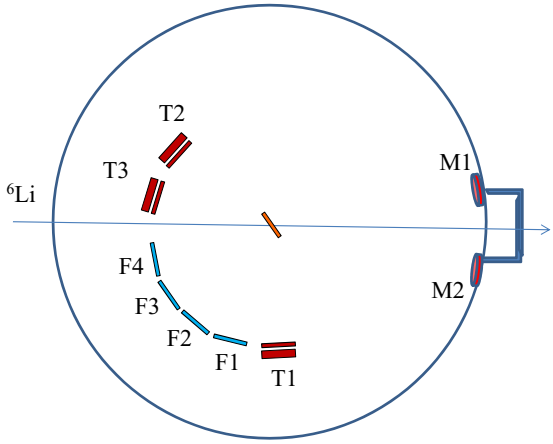

FIG. 1. Schematic diagram of the experimental setup inside scattering chamber with four single silicon strip detectors (F_1–F_4) to detect fission fragments, three telescopes (T_1–T_3) made of $\Delta E - E$ silicon strip detectors to detect light charged particles, and two monitor detectors (M_1 and M_2).

drawn in Fig. 2(a) to separate the events lying to the right of this line with higher energies corresponding to fission and the events lying to the left of this line corresponding to the projectile-like fragments (PLFs).

To measure the PLFs, three telescopes, T_1–T_3, have been used. Each of these telescopes ($\Delta E - E$) is made of two silicon strip detectors of same size as mentioned earlier. The thicknesses of ΔE detectors are ∼50–60 μm and those of E detectors are ∼1500 μm. One of the telescopes, T_1, with an angular coverage of ∼72–88°, was mounted on the same (fixed) arm where fission detectors were mounted. The other two telescopes, T_2 and T_3, having a combined angular coverage of ∼36°, were placed on another arm, which is rotatable and kept on the other side of the beam. These detectors were placed around the grazing angles to obtain good coincidence statistics while investigating the transfer or breakup effect on inclusive FF angular distribution. They were also placed at nongrazing angles (i) to find out the dependence of FF angular anisotropy on the angle of PLF emission if any and (ii) to measure the angular distributions of outgoing α, d, and p.

Data were first recorded in singles mode to measure the inclusive fission-fragment angular distribution and then in coincidence mode to measure the breakup- or transfer-induced fission angular distribution. For coincidence mode, the fission fragment detected in any of the fission detectors (F_1 OR F_2 OR F_3 OR F_4) is recorded when there is a simultaneous light charged particle detected in any of the three telescopes (T_1 OR T_2 OR T_3) to get the breakup- or transfer-induced fission yield.

Typical two-dimensional ($\Delta E - E_{\text{total}}$) spectrum for light charged particles (with atomic numbers $Z = 1$, 2, and 3) obtained from 16 strips of T_3 in coincidence mode is shown in Fig. 2(b). E_{total} was obtained by adding the ΔE and E_{res} signals after gain matching and energy calibration. The one-dimensional projection of α band as selected by a two-dimensional gate in the above figure on E_{total} axis is shown in Fig. 2(c). The velocity corresponding to the energy of the α peak was found to be equal to the beam velocity,

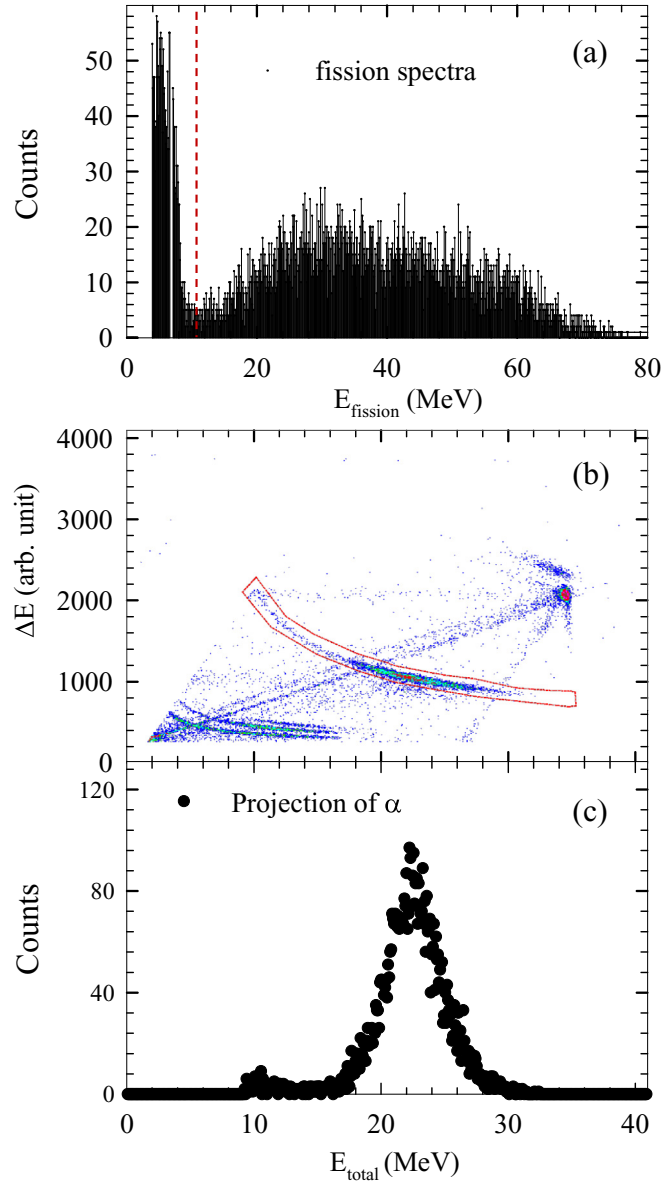

FIG. 2. (a) Typical spectrum of fission fragments detected in one of the 16 strips of F_3 fission detector in coincidence with the projectile-like fragments in any of the three telescopes (T_1 OR T_2 OR T_3) at $E_{\text{beam}} = 36$ MeV, (b) typical two-dimensional ($\Delta E - E$) raw spectrum for light charged particles ($Z = 1$–3) detected by T_3 telescope in coincidence with fission fragments in any of the four fission detectors (F_1 OR F_2 OR F_3 OR F_4), and (c) one-dimensional projection of α band, selected from the above two-dimensional plot, on the x axis.

suggesting that most of the α particles are originated from the projectile breakup.

III. INCLUSIVE FISSION FRAGMENT ANGULAR DISTRIBUTION

Inclusive fission-fragment angular distributions $W_{\text{lab}}(\theta_{\text{lab}})$ were obtained from the fission yields detected in the fission detectors in singles mode for three near-barrier bombarding

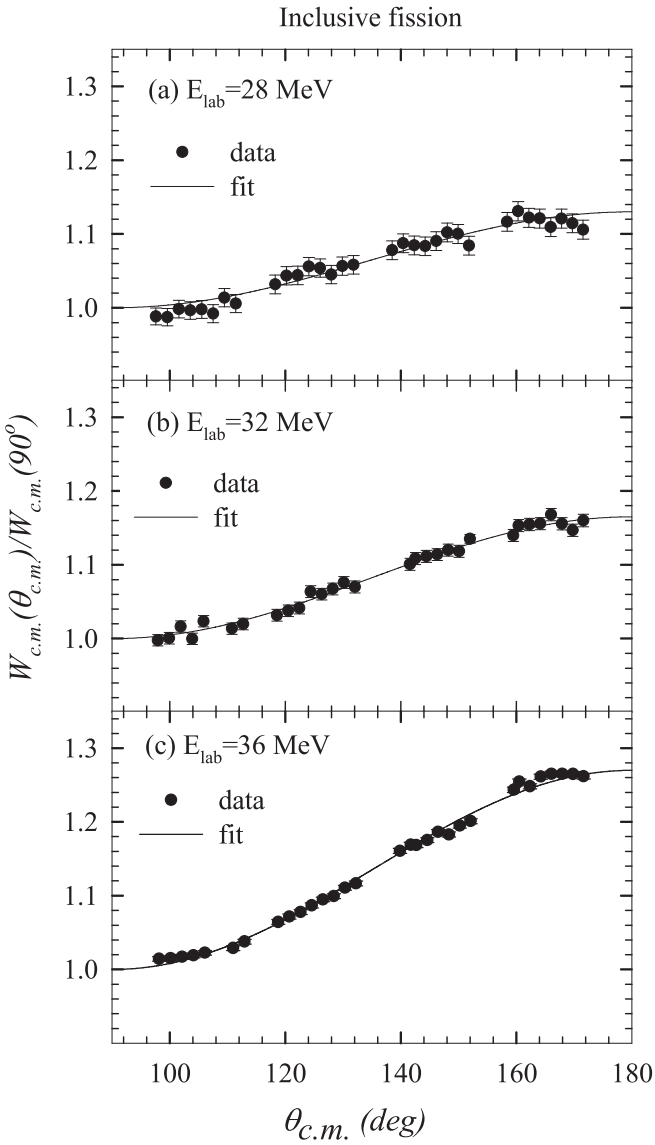

FIG. 3. Inclusive (total) fission fragment angular distribution at beam energies of (a) 28, (b) 32, and (c) 36 MeV.

energies, $E_{\rm beam} = 28$, 32, and 36 MeV. Yields from two adjacent strips of fission detectors have been combined together to improve the statistics. The measured distributions have been transformed to the center-of-mass system using the well-known expression [26]

$$W_{\rm c.m.}(\theta_{\rm c.m.}) = W_{\rm lab}(\theta_{\rm lab})\frac{1 + x\cos(\theta_{\rm c.m.})}{(1 + 2x\cos(\theta_{\rm c.m.}) + x^2)^{3/2}}, \quad (1)$$

where x is the ratio of center-of-mass velocity $v_{\rm c.m.}$ to the velocity of fission fragments in center-of-mass frame v_f (i.e., $x = \frac{v_{\rm c.m.}}{v_f}$). The value of v_f has been calculated from Viola's systematics for fragment kinetic energies [27]. The center-of-mass angle is calculated using the relation $\theta_{\rm c.m.} = \theta_{\rm lab} + x\sin\theta_{\rm lab}$. The inclusive FF angular distributions in center-of-mass frame thus obtained at $E_{\rm lab} = 28$, 32, and 36 MeV are shown as solid circles in Figs. 3(a)–3(c) respectively.

TABLE I. Fission fragment angular anisotropy for total (inclusive) fission.

Energy (MeV)	Anisotropy (inclusive)
28	1.13 ± 0.04
32	1.16 ± 0.03
36	1.27 ± 0.02

The angular distribution data in center-of-mass frame have been fitted using the expression $W(\theta) = a_0 + a_2\cos^2\theta$. From the fitted curves, shown as solid lines in Fig. 3, the ratio $W(180^\circ)/W(90^\circ)$ has been calculated to obtain the FF angular anisotropy of the respective angular distributions, which are tabulated in Table I. The above anisotropy values, shown by filled circles in Fig. 4, are found to be within the experimental errors of the existing data (hollow circles) measured by Freiesleben *et al.* [15]. However, the central anisotropy values for the present data are slightly higher than the ones from the literature. Anisotropy values from the present measurement as well as from Ref. [15] are in general found to be higher compared to the SSPM predictions as shown by a solid line in Fig. 4.

Based on SSPM formalism, the anisotropy A has been calculated as $A = 1 + \frac{\langle \ell^2 \rangle}{4K_0^2}$, where $\langle \ell^2 \rangle$ was derived from the σ_ℓ versus ℓ distribution obtained from CCDEF code [28]. The input parameters of CCDEF are constrained by the fission excitation function available in the literature. The potential parameter with $DV = 40.0$ and target deformation parameters with $\beta_2(^{232}\text{Th}) = 0.22$ and $\beta_4(^{232}\text{Th}) = 0.09$ [29] have been used. The variance of the K distributions is $K_0^2 = I_{\rm eff}T/\hbar^2$. Here, $I_{\rm eff}$ is the effective moment of inertia and $T = \sqrt{(E^*/a)}$ is the

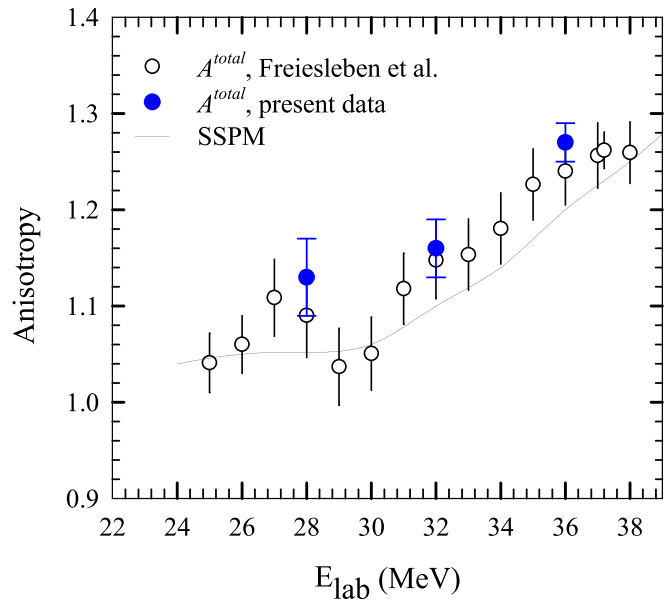

FIG. 4. Fission-fragment angular anisotropy for inclusive fission obtained from the present data (filled circle) and the existing data by Freiesleben *et al.* [15] (hollow circle) are compared with SSPM calculations (solid line) at near-barrier energies.

saddle-point temperature of the compound nucleus. The level density of the compound nucleus of mass A_{CN} is taken to be $a = A_{CN}/10$ MeV^{-1}. The excitation energy E^* at the saddle point is given by $E^* = E_{\text{c.m.}} + Q - B_f - E_{\text{rot}} - E_n$, where Q is the Q value for the formation of the compound nucleus. The spin-dependent fission barrier B_f, ground-state rotational energy E_{rot}, and effective moment of inertia I_{eff} are calculated using the Sierk model [30]. E_n is the average energy removed by the evaporated neutrons from the compound nucleus [31]. The average number of pre-scission neutrons was found to be in the range of 0.65–1.68 for the beam energy 24–40 MeV.

IV. BREAKUP- OR TRANSFER-INDUCED FISSION-FRAGMENT ANGULAR DISTRIBUTIONS

The anisotropy of the breakup-induced fission fragments can be extracted using the measured yields of fission fragments in coincidence with projectile breakup fragments like α, deuteron, and proton. In an incomplete fusion reaction, the composite nucleus formed by the capture of a breakup fragment and the complementary breakup fragment of the projectile start moving simultaneously at certain angles with respect to the beam direction. The recoil direction of the composite system will depend upon the angle and momentum of the outgoing projectile-like fragment (PLF). The direction of the recoiled composite nuclei and the corresponding angles of the fission fragments with respect to the recoil direction were calculated event by event to obtain the actual FF angular distributions with respect to an average recoil direction. To obtain the transfer- or breakup-induced FF angular distributions $Y'(\theta')$ in the rest frame of the recoiling nuclei, the following conversions have been used. Here, θ' is the angle of fission fragments in the rest frame of recoiling nuclei which is calculated as

$$\theta' = \theta'' + y\sin(\theta''), \tag{2}$$

where θ'' is the angle in the laboratory frame between the direction of the fission-fragment emission (θ_{fission}) and the direction of the recoil of the composite nucleus formed by the capture of the breakup fragment by the target (θ_{recoil}), i.e.,

$$\theta'' = \theta_{\text{fission}} - \theta_{\text{recoil}}, \tag{3}$$

and y is equal to the ratio of recoil velocity of the residue nuclei v_{rec} to the velocity of fission fragment v_f, i.e., $y = \frac{v_{\text{rec}}}{v_f}$.

In the rest frame of recoiling nuclei, the solid angle transformation for the FF angular distribution is given by

$$Y'(\theta') = Y''(\theta'')\frac{1 + y\cos(\theta')}{[1 + 2y\cos(\theta') + y^2]^{3/2}}, \tag{4}$$

where $Y''(\theta'')$ is the FF angular distribution in the laboratory frame with respect to recoil direction.

A. Fission in coincidence with α

The most dominant channel for the transfer- or breakup-induced fission was found to be the channel producing fission in coincidence with α. The breakup- or transfer-induced FF angular distribution $Y''(\theta'')$ has been obtained with respect to average recoil angle for two different situations corresponding to the detection of FF in coincidence with the α emitted (i) at forward angles and (ii) at backward angles. These two distributions will bring out any dependence of FF angular anisotropy on the angle of the α emission. To detect the α, the telescope T_3 was placed once at forward angle and then at backward angle covering the angular ranges of 72–88° and 154–170° respectively. To limit the range of recoil angles, coincident counts of only 8 central strips of T_3 have been used for obtaining the FF angular distributions. The variation in the corresponding recoil angle of the composite nucleus was found to be within ±3°.

In the first case, the telescopes T_1 and T_3 were placed at symmetric positions on either side of the beam, in the angular range of ±(72–88°), to get the angular anisotropy with respect to forward-moving α. For a typical beam energy of $E_{\text{beam}} = 36$ MeV, when α is detected at T_3, which is placed on the left side of the beam, the recoil direction is on the right side of the beam, and the average recoil angle with respect to the beam direction is calculated to be $\theta_{\text{recoil}} \approx +35°$. Thus, with respect to the recoil direction, the FF angular distribution covers the angular range of $\theta'' \sim 59$–$138°$. Simultaneously, when α gets detected at T_1, which is placed on the right side of the beam, the recoil direction is on the left side of the beam direction with $\theta_{\text{recoil}} \approx -35°$ leading to the FF angular distribution range of $\theta'' \sim 129$–$208°$. Hence, using data of both T_1 and T_3, the FF angular distribution in the rest frame of recoiling nuclei could be measured in the angular range of $\theta'' \sim 59$–$208°$. Similarly, the angular distribution of fission fragments measured in coincidence with α for $E_{\text{beam}} = 32$ MeV was obtained. The resultant FF angular distributions after transformation to the rest frame of the recoil nuclei are shown as open circles in Fig. 5 for (a) 32 and (b) 36 MeV. The measured FF angular distributions were fitted by the expression $Y'(\theta') = a_0 + a_2\cos^2\theta'$ (solid lines) to obtain the angular anisotropy at two energies. For $E_{\text{beam}} = 28$ MeV, the coincidence yields of outgoing α particles detected at the telescopes T_1 and T_3 are less as they are placed at 72–88°, which is far from the grazing angle (∼180°). So, the FF angular distribution was not obtained at this energy. The angular anisotropy obtained for 32 and 36 MeV are 1.16 ± 0.04 and 1.17 ± 0.03 respectively.

For the second case (backward-moving α), i.e., when α gets detected by T_3 telescope placed in the angular range 154–170°, the average recoil angle $\theta_{\text{recoil}} \approx +10°$. The fission yield in coincidence with α detected in T_3 telescope only has been used to obtain the FF angular distribution in the rest frame of recoiling nuclei, which are shown as filled circles in Fig. 6. The measured FF angular distributions were fitted by the expression $Y'(\theta') = a_0 + a_2\cos^2\theta'$ (solid line) and angular anisotropies obtained for 28, 32, and 36 MeV, respectively, are 1.26 ± 0.04, 1.16 ± 0.04, and 1.23 ± 0.03.

Comparing the above results, it was found that the FF anisotropy is the same (within the experimental errors) for the two cases. Hence, it can be assumed that the anisotropy is independent of the direction of the emission of the α, or alternately, it is independent of the recoil direction of the residual fissioning nuclei. The average values of the anisotropy obtained from the two cases for α-gated fission fragments are found to be 1.26 ± 0.04, 1.16 ± 0.04, and 1.20 ± 0.04

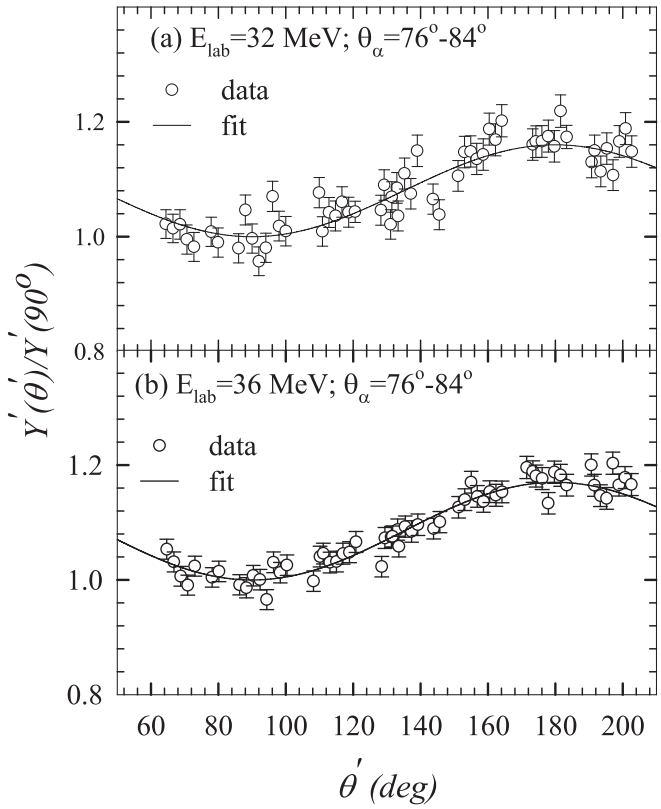

FIG. 5. Angular distributions of α-gated fission fragments in the rest frame of the recoil nuclei for the beam energies of (a) 32 MeV and (b) 36 MeV when α is detected in the forward angles.

for $E_{\rm beam} = 28$, 32, and 36 MeV respectively. These values have been used in Sec. V B to obtain the overall contributions corresponding to all possible values of $\theta_{\rm PLF}$.

B. Fission in coincidence with deuteron and proton

Interestingly, there is a significant yield of fission fragments detected in the fission detectors in coincidence not only with deuterons but also with protons observed in telescopes T_1 and T_2. Like in the previous subsection, the yields of fission fragments detected in fission detectors in coincidence with the deuterons and protons detected in the telescopes have been extracted. The statistics for deuteron- and proton-gated fission for $E_{\rm beam} = 28$ MeV was poor. So, for remaining two beam energies, $E_{\rm beam} = 32$ and 36 MeV, the angular distributions of the fission fragments in coincidence with deuterons and protons have been obtained in the frame of recoil nuclei and are shown in Figs. 7 and 8 respectively. Using the fit by the expression $Y'(\theta') = a_0 + a_2\cos^2\theta'$, the FF angular anisotropies for deuteron- and proton-gated fissions have been obtained.

A comprehensive list of in-plane fission fragment angular anisotropy for breakup-induced fissions gated with α, d, and p in the rest frame of recoiling nuclei has been given in Table II. It was interesting to observe that some of the anisotropy values, particularly for d-gated and p-gated fissions, in the rest frame of recoiling nuclei are stronger than those for the inclusive fission in center-of-mass frame. While the in-plane anisotropy for α-gated fission is found to be higher at $E_{\rm beam} = 28$ MeV,

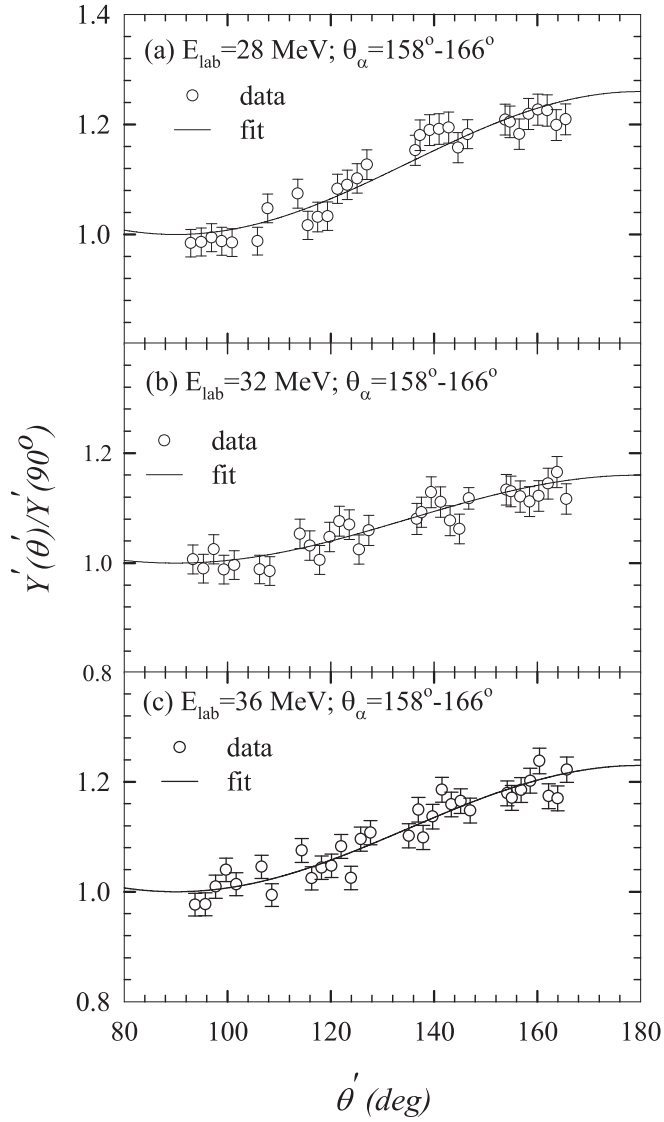

FIG. 6. Angular distributions of α-gated fission fragments in the rest frame of the recoil nuclei for the beam energies of (a) 28 MeV, (b) 32 MeV, and (c) 36 MeV when α is detected at the backward angles.

it is smaller at $E_{\rm beam} = 36$ MeV with respect to the ones for inclusive fission at respective energies.

However, these anisotropy values may not give the exact picture of how the overall anisotropy due to breakup- or transfer-induced fission affects the anisotropy of the inclusive total fission, because these FF angular distributions have been obtained in coincidence with light charged particles detected only in limited solid angles in a reaction plane. Second, the contribution to the overall anisotropy for total fission will depend on the individual probabilities of different breakup- or transfer-induced fission channels.

V. EFFECT OF PROJECTILE BREAKUP ON INCLUSIVE FISSION

One of the motivations of the present work is to investigate the effect of projectile breakup, if any, on the FF angular

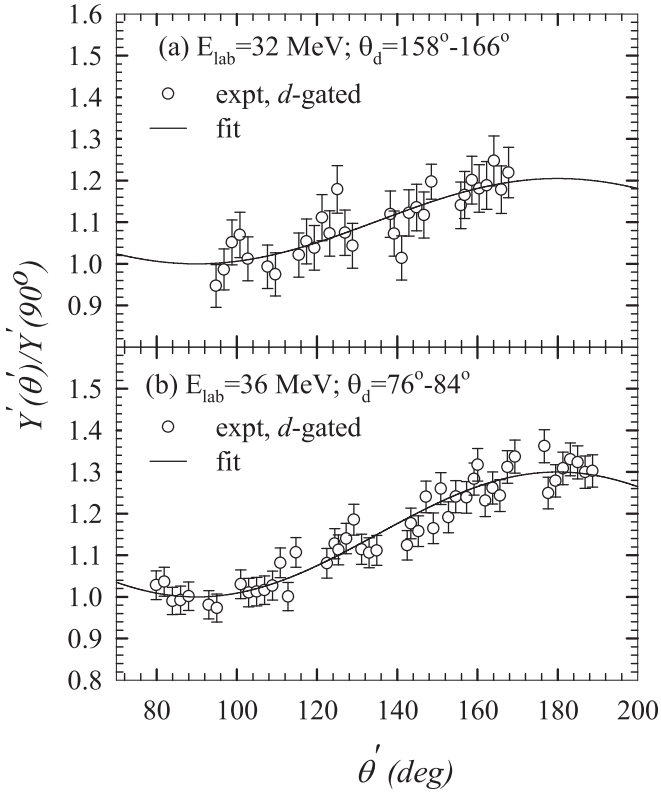

FIG. 7. Angular distribution for fission fragments measured in F_1–F_4 detectors in coincidence with deuterons detected by the telescopes in the angular range of (a) 158–166° for $E_{beam} = 32$ MeV and (b) 76–84° for $E_{beam} = 36$ MeV.

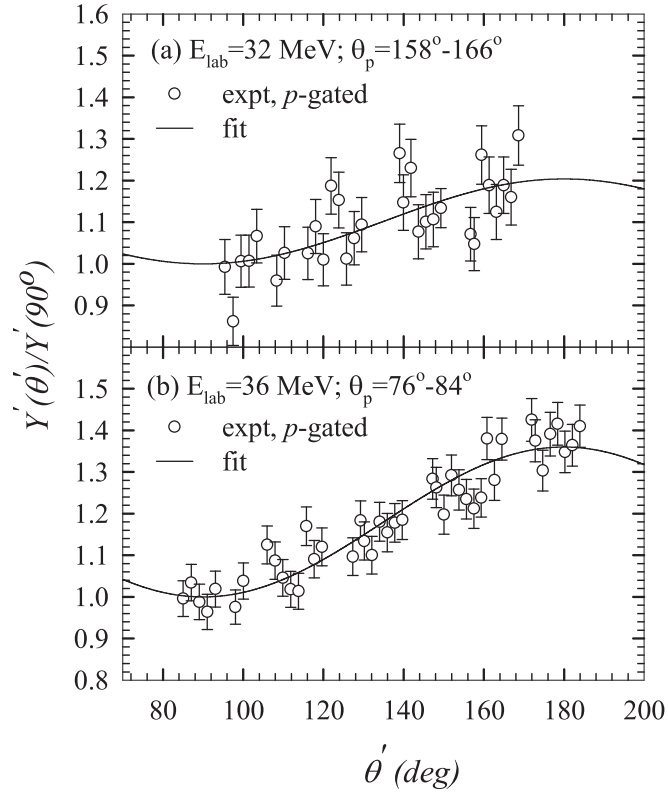

FIG. 8. Angular distribution for fission fragments measured in F_1–F_4 detectors in coincidence with protons detected by the telescopes in the angular range of (a) 158–166° for $E_{beam} = 32$ MeV and (b) 76–84° for $E_{beam} = 36$ MeV.

anisotropy of inclusive fission. In order to obtain the overall anisotropy of the FF angular distribution correlated with the PLFs emitted in all solid angles, the knowledge of both in-plane and out-of-plane anisotropies is essential. However, as mentioned in the introduction and observed in Refs. [19,25], for beam energies near and below the Coulomb barrier where grazing angles are in backward directions, the out-of-plane correlations between FFs and PLFs are expected to be isotropic. For the present measurements at low energies, especially at 28 and 32 MeV, the isotropic correlations may be assumed. In other words, the angular distribution with respect to the direction of the recoiling heavy nucleus is symmetric. Thus, the overall effect of breakup-induced fissions can be obtained by using their in-plane anisotropy only. It may be recollected that the present experimental setup is consisted of detectors for both FFs and PLFs placed in the same plane that provides the in-plane correlation.

The FF angular anisotropies of the breakup-induced fission fragments measured in coincidence with α, deuteron, and proton that are emitted in the same plane have already been extracted in the previous section. However, due to limited coverage of the light charged particle detectors, even in the reaction plane itself, the above anisotropy does not provide the correct representation of the effect of breakup on the inclusive fission-fragment angular anisotropy. To study the overall effect, one needs to find out the contributions of breakup-induced fissions corresponding to all possible laboratory angles (θ_{PLF}) of the outgoing complementary projectile breakup fragments emitted in the same plane in coincidence with fission fragments with proper weight factor $P(\theta_{PLF})$. This weight factor is proportional to the differential cross sections of the outgoing projectile-like fragments. For each angle of the light charged particles with an average momentum, there is a corresponding recoil angle (θ_{recoil}) of the composite nuclei formed by the capture of the complementary breakup fragments by the target nuclei.

To find the effect of breakup-induced fission on the angular anisotropy of the total fission, the following procedure has been followed. First, the experimental angular distribution of breakup-induced fission fragments was obtained in the rest frame of recoiling nuclei. Second, the angular distributions $d\sigma(\theta_{PLF})/d\Omega$ were obtained for the outgoing projectile breakup

TABLE II. Fission fragment angular anisotropy (A) for breakup or transfer induced fissions gated with α, d, and p in the frame of recoil nuclei.

Energy (MeV)	A (α-gated)	A (d-gated)	A (p-gated)
28	1.26 ± 0.04		
32	1.16 ± 0.04	1.21 ± 0.09	1.20 ± 0.24
36	1.20 ± 0.04	1.30 ± 0.08	1.36 ± 0.08

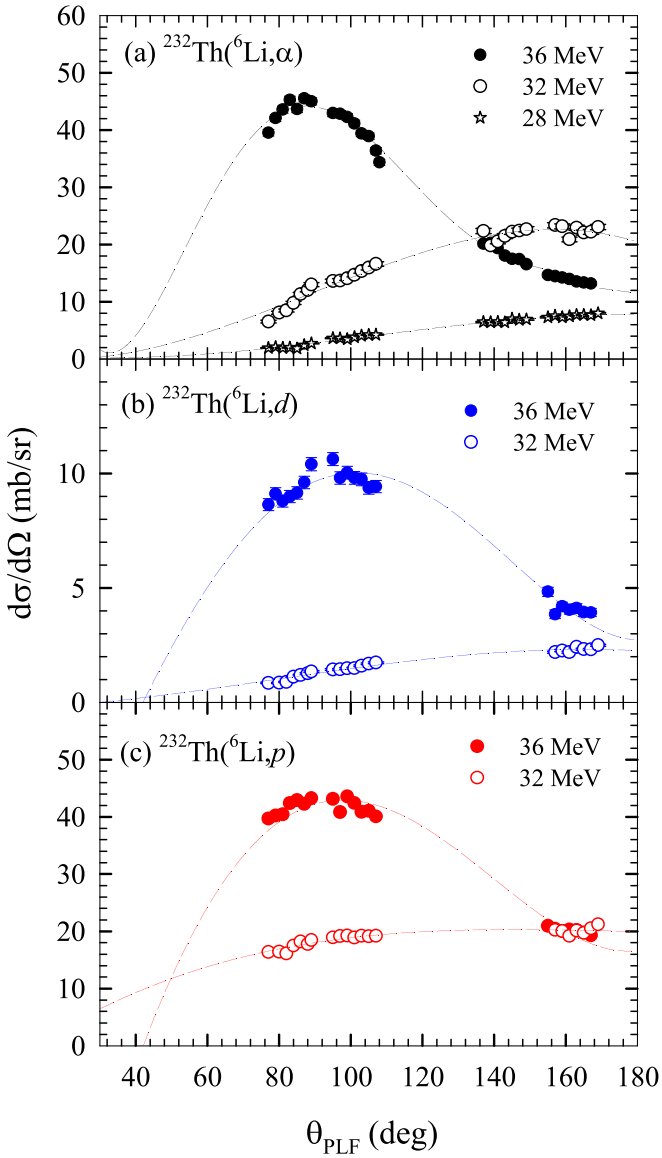

FIG. 9. Differential cross sections for (a) inclusive α at $E_{\rm beam} =$ 28, 32, and 36 MeV, (b) inclusive deuteron at $E_{\rm beam} = 32$ and 36 MeV, and (c) inclusive proton at $E_{\rm beam} = 32$ and 36 MeV, produced in the ^{6}Li + ^{232}Th reaction.

fragments like α, d, and p to find the weight factors $P(\theta_{\rm PLF})$ mentioned above. Third, the overall angular distribution of breakup-induced fission fragments was obtained by integrating the contributions corresponding to all possible angles of PLF emissions with weight factor $P(\theta_{\rm PLF})$.

A. Angular distributions of outgoing α, d, and p

Inclusive yields for α, d, and p have been extracted from the data recorded by the telescopes in singles mode. Angular distributions for α, d, and p productions obtained from these yields are shown in Fig. 9. The cross sections for inclusive α produced in the present reaction at $E_{\rm beam} = 28$, 32, and 36 MeV are shown in Fig. 9(a) as stars, open circles, and filled circles respectively. Dashed lines represent the fits to the experimental data.

Similarly, the experimental differential cross sections for inclusive deuterons and protons produced in the present reaction have been shown in Figs. 9(b) and 9(c) respectively. The data for $E_{\rm beam} = 32$ and 36 MeV have been represented by open and filled circles respectively. Dashed lines represent the fits to the data that are used to obtain the weight factor $P(\theta_{\rm PLF})$ at any angle $\theta_{\rm PLF}$. The cross sections of protons and deuterons at $E_{\rm beam} = 28$ MeV have not been shown in the figure, as statistics of the fission fragments detected in coincidence with d and p at these two beam energies were very poor.

B. Overall anisotropy for breakup-induced fission

As mentioned earlier, the overall effect of breakup-induced fission on inclusive fission-fragment angular anisotropy can be found only when one considers all the fission events detected in coincidence with light charged particles emitted in all possible solid angles. However, for the case of isotropic emission of correlated PLFs and FFs out of plane, the in-plane anisotropy becomes important. In the present measurement, the grazing angles at $E_{\rm beam} = 28$, 32, and 36 MeV are $\sim$180°, 160°, and 90°, respectively, which are not in forward angles. Similar to the one observed in Refs. [19,25] for ^{16}O + ^{232}Th and d + ^{239}Pu reactions, one can expect that the out-of-plane distributions at lower energies for the present system with grazing angles in backward directions, especially for 28 and 32 MeV, are isotropic. In such cases, the in-plane anisotropy in transfer- or breakup-induced fissions plays an important role in modifying the inclusive FF angular anisotropy.

However, to account for all transfer events including those where the projectile-like fragment has not been observed, one has to realize that the directions of recoils, beam axis, and a fission fragment will not generally be situated in the same plane. The recoils should be allowed to go out of plane, and one must then average over recoil directions out of plane, for given recoil angle with respect to the beam axis. As shown in the appendix, this can be carried out by applying spherical harmonics algebra and arriving at a very simple expression. The angular distribution of breakup- or transfer-fission in the frame of recoil nuclei has been assumed to be independent of the direction of recoil. The overall effect of breakup-induced fission due to all possible recoil angles both in and out of plane can thus be inferred using the in-plane angular distribution only. By averaging over all the recoil angles ($\theta_{\rm recoil}$), the angular distribution in the rest frame of recoil nuclei with respect to beam axis can be obtained as

$$W(\theta_{\rm fission}) = 1 + A_2 P_2(\cos\theta_{\rm recoil}) P_2(\cos\theta_{\rm fission}). \quad (5)$$

Here, the angular distribution coefficient has just been multiplied by a factor $P_2(\cos\theta_{\rm recoil})$ that accounts the contribution from all out-of-plane recoil angles. Once this extra factor is included, the effect of out-of-plane recoils is incorporated while considering the $\theta_{\rm PLF}$, $\theta_{\rm recoil}$, and $\theta_{\rm fission}$ to be in the same reaction plane.

To obtain the overall angular distribution, the following steps have been followed. First, the angular distribution of

breakup- or transfer-induced fission in the frame of recoil nuclei obtained in the previous section was assumed to be independent of the direction of recoil. This is a valid assumption because the difference in the FF anisotropy corresponding to fission in coincidence with forward-moving α and backward-moving α was not significant compared to the experimental error as observed in Figs. 5 and 6. For the case of α-gated FF angular distribution in recoil frame, at $E_{\rm beam} = 32$ and 36 MeV, the average shape of the two angular distributions was assumed to be independent of recoil direction. And for the other cases, the FF angular distributions measured in coincidence with the PLFs detected around the grazing angles were used as representative angular distributions for all the recoil directions.

Now, for a fixed $\theta_{\rm recoil}$, the above distribution of $W(\theta_{\rm fission})$ in the rest frame of recoil nucleus can be converted into the distribution in the laboratory frame $[Y_{\rm lab}(\theta_{\rm lab})]$. These distributions were then multiplied by a corresponding weight factor $P(\theta_{\rm PLF})$. Sum of these weighted angular distributions, i.e., $\Sigma_{\theta_{\rm PLF}} Y_{\rm lab}(\theta_{\rm lab}) P(\theta_{\rm PLF})$, is the overall breakup or transfer fission angular distribution in laboratory frame with respect to the beam axis corresponding to each of the outgoing channels at the measured energies. These angular distributions were finally converted to the center-of-mass frame distribution $Y_{\rm c.m.}(\theta_{\rm c.m.})$, as shown in Fig. 10. The solid, dashed, and dash-dotted lines represent the estimated overall angular distributions corresponding to the fission fragments emitted in coincidence with p, d, and α respectively.

The final anisotropy of the above overlapping distributions considering both in- and out-of-plane recoils obtained for α-, deuteron-, and proton-gated fission events at various energies have been tabulated in Table III.

The estimated anisotropy of breakup-induced fission in coincidence with both in- and out-of-plane α (the dominant channel) is less than or equal to the ones observed for the inclusive fission fragments. For d- and p-gated fission fragments, the angular anisotropy values are found to be slightly higher but within the experimental errors of inclusive fission. In the present measurements, since the dominant breakup-induced fissions are the ones measured in coincidence with α particles, the overall in-plane anisotropy of the breakup or transfer fission will be less than or equal to the total anisotropy. Therefore, the anisotropy corresponding to pure CF fission could actually be more than the anisotropy observed for the total fission. This will further enhance the difference in the anisotropy between SSPM prediction and the ones for pure CF fission.

So it can be concluded that the observed enhancement in the anisotropy for total fission compared to the SSPM predictions at near-barrier energies is not due to the contribution from breakup- or transfer-induced fissions. However, it may be emphasized that the above conclusion is true only when the out-of-plane correlation is isotropic.

Further measurements of fission fragments in coincidence with the PLFs emitted in all possible solid angles using both in-plane and out-of-plane detectors are necessary to confirm the above picture of the FF angular anisotropy corresponding to the breakup- or transfer-induced fission.

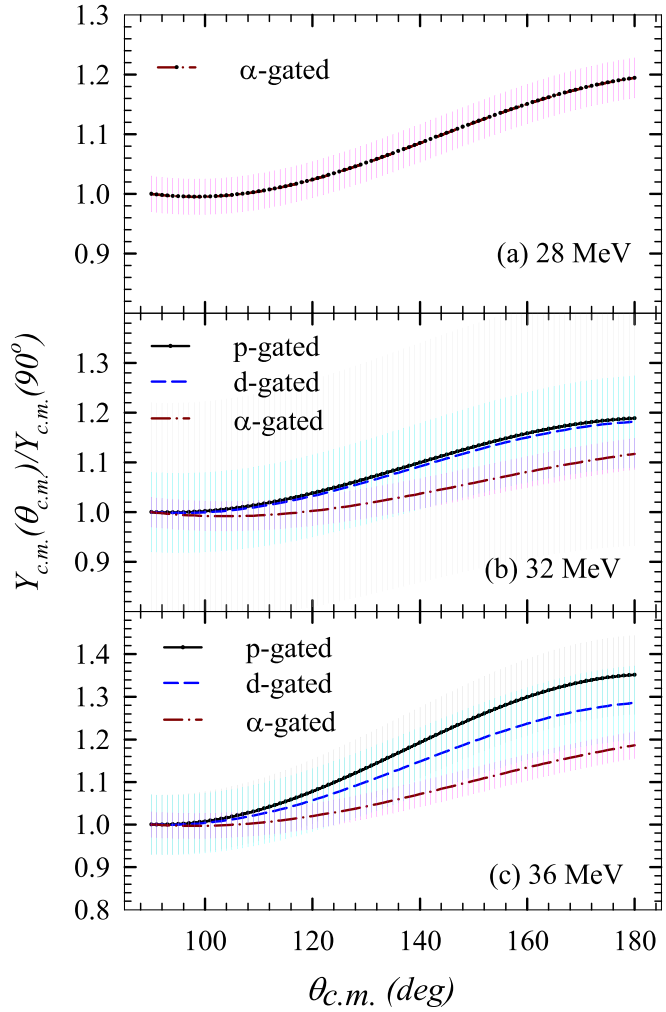

FIG. 10. Estimated overall angular distributions of breakup- or transfer-induced fission fragments in coincidence with p, d, and α emitted in all possible directions, with respect to the beam axis in the center-of-mass frame.

VI. PRE-EQUILIBRIUM FISSION

The enhancement of experimental FF angular anisotropy compared to SSPM predictions can be understood in terms of a pre-equilibrium fission (PEF) model based on the entrance-channel-dependent (ECD) K-state distribution [32–34]. If the input K distribution is not fully equilibrated, the PEF mechanism can lead to anomalous fission-fragment anisotropies.

TABLE III. Overall fission-fragment angular anisotropy A in the center-of-mass frame due to the breakup- or transfer-induced fissions gated with α, d, and p emitted in as well as out of plane compared to inclusive total fission.

Energy (MeV)	A (inclusive)	A (α-gated)	A (d-gated)	A (p-gated)
28	1.13 ± 0.04	1.19 ± 0.04		
32	1.16 ± 0.03	1.12 ± 0.04	1.18 ± 0.09	1.19 ± 0.24
36	1.27 ± 0.02	1.19 ± 0.04	1.29 ± 0.08	1.35 ± 0.08

For many reactions involving actinide targets, the contribution from PEF along with compound nucleus fission have been observed, particularly at sub- and near-barrier energies. In the cases of ^{10,11}B + ^{232}Th [29], ^{10,11}B + ^{237}Np [35], and ^{6,7}Li + ^{235,238}U [17] systems, the experimental anisotropy values have been explained by the ECD pre-equilibrium fission model with the incorporation of the effect of ground-state spin of the target and projectile (S).

The PEF model calculations were performed for the present system to understand the measured anisotropy. Here, the K distribution has been modified to incorporate the entrance channel ground-state spin of the target and projectile as given below:

$$F(J,K,K') = \exp\left[\frac{-(K-K')^2}{2\sigma_K^2}\right] \times \exp\left[\frac{-K^2}{2K_0^2}\right],$$

where $K' = J\sin\omega \pm S$ and $\sigma_K = qJ\sqrt{Tt}$ with t being the Bohr-Wheeler fission time and q being a constant obtained from the fit to the experimental data. T is the temperature of the compound nucleus and K_0^2 is the variance of the K distribution. The entrance channel K-state population for a particular angular momentum value J and ω decides the fusion cross section $\sigma_{\rm fus}(J,\omega)$ for the angular momentum value J at various target projectile orientations ω. Now the modified angular distribution is given by

$$W(\theta) \propto \Sigma_{J=0}^{\rm Jmax}\Sigma_{M=-S}^{S}\Sigma_{\omega}\sigma_{\rm fus}(J,\omega) \times \frac{\Sigma_{K=-J}^{J}(2J+1)\left|d_{M,K}^{J}(\theta)\right|^2 F(J,K,K')}{\Sigma_{K=-J}^{J}F(J,K,K')}.$$

Here, $d_{M,K}^{J}(\theta)$ is the rotational wave function [36]. The orientation-dependent partial cross sections $\sigma_{\rm fus}(J,\omega)$ for the present system have been calculated using the coupled-channels code for fusion, CCDEF [28]. Using the above expressions and including the ground-state spins of the projectile and target, the FF angular distributions. i.e., $W(\theta)$ have been calculated at different energies. The results for corresponding FF angular anisotropy are shown in Fig. 11 as a solid line. The anisotropy values obtained from the ECD K-state distributions are larger than the SSPM values (dashed lines) and they reproduce the measured values reasonably well. The parameter q has been adjusted to 0.12 (MeV $\times$ 10^{-21} s)$^{-1/2}$ (slightly smaller than the value used in Ref. [29] for ^{10,11}B + ^{232}Th reactions) to reproduce the measured anisotropy data, assuming the discrepancy between the SSPM anisotropy and experiment is totally due to pre-equilibrium fission. Hence, the PEF alone can explain the deviation in observed anisotropy for total fission from SSPM prediction.

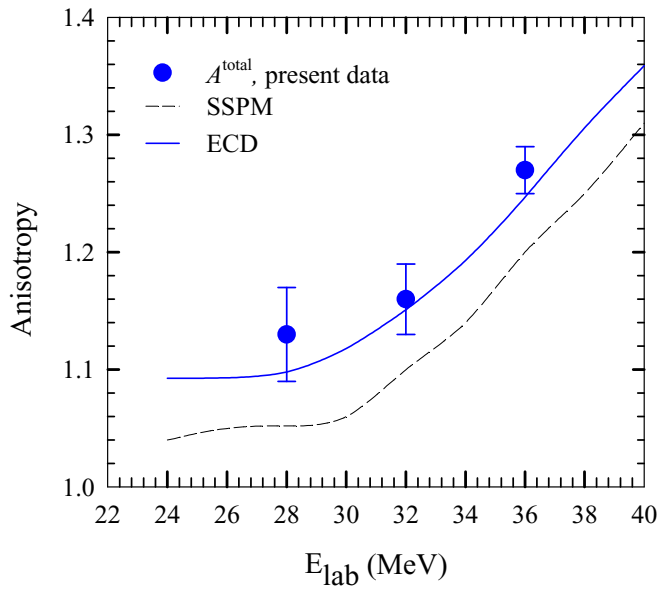

FIG. 11. Fission-fragment angular anisotropy for total fission obtained from present data (filled circle) are compared with the calculations using ECD K-state model (solid line) at near-barrier energies.

VII. SUMMARY

Inclusive and exclusive FF angular distributions have been measured at three near-barrier projectile energies, i.e., 28, 32, and 36 MeV for ^{6}Li + ^{232}Th system. The FF angular anisotropy obtained from the measured inclusive data were found to lie within the experimental errors of the existing values [15], though the central values of the present anisotropies are slightly higher. Inclusive FF angular distribution consists of both CF and ICF fission events. To disentangle the angular anisotropies of ICF fissions from CF fission, the fission fragments were measured in coincidence with outgoing projectile breakup fragments like α, deuteron, and proton in the reaction plane, and the corresponding FF angular anisotropies in the rest frame of the recoiling nuclei were obtained. The α-gated fission reaction was found to be the major ICF-induced fission channel. Interestingly, some of the anisotropies of transfer-induced (e.g., p-gated and d-gated) fission in the rest frame of recoiling nuclei were found to be stronger than the respective anisotropies for inclusive FFs in the center-of-mass frame.

The overall angular anisotropy for the exclusive fission events in coincidence with α particles emitted in all possible directions within and out of the reaction plane were estimated to be smaller than or equal to that of the inclusive fission for all three beam energies. The FF angular anisotropy corresponding to the deuteron-gated and proton-gated fission were found to be slightly more than the α-gated fission but they are within the experimental errors of the inclusive fission. Therefore, assuming isotropic out-of-plane angular correlations as observed in Refs. [19,25], it may be concluded that the breakup-induced fission channels are not contributing to the enhancement of total anisotropy compared to the theoretical SSPM predictions. However, further measurements using PLF detectors both in as well as out of the reaction plane are necessary to obtain an exact angular distribution of transfer- or breakup-induced fission and confirm the above conclusion.

The observed anisotropy for total fission at near-barrier energies could be explained in terms of entrance-channel-dependent pre-equilibrium fission model, implying that the contribution from pre-equilibrium fission along with compound nucleus fission may be one of the reasons behind the

enhanced anisotropy for total fission compared to the SSPM prediction.

ACKNOWLEDGMENTS

We would like to thank the Pelletron crew for the smooth operation of the accelerator during the experiments. Thanks are also due to Dr. K. Mahata for many useful discussions during the preparation of the manuscript.

APPENDIX

The angular distribution of fission with respect to the rest frame of recoil nuclei, as measured in the reaction plane, can be written in terms of a second-order Legendre polynomial P_2 as

$$W(\theta') = 1 + A_2 P_2(\cos\theta'). \quad \text{(A1)}$$

(This is equivalent to writing $1 + a\cos^2\theta'$, and one can relate the coefficients and the normalization of the two expressions to each other). Earlier measurements on transfer-induced fission show that it is a very good approximation to let this angular distribution be valid irrespective of whether the fission fragments are emitted in the reaction plane or not. However, to estimate the contribution to fission from all transfer events, irrespective of whether the projectile-like fragment has been observed or not, one has to consider all directions of the recoiling nucleus for a particular value of recoil angle θ_{recoil} relative to the beam axis (see Fig. 12). Thus, one must average over (i) Φ_{recoil} (the small circle making a solid angle sphere indicated by the dash-dotted blue curve in Fig. 12) for a particular θ_{recoil} centered at the beam axis, and then over (ii) θ_{recoil} with appropriate weight factor. Now, one can apply the relation for spherical harmonics, in this case for $\ell = 2$:

$$P_\ell(\cos\theta') = \frac{4\pi}{2\ell+1}\sum_m Y^*_{2m}(\theta_{\text{recoil}}, \Phi_{\text{recoil}}) \times Y_{2m}(\theta_{\text{fission}}, \Phi_{\text{fission}}).$$

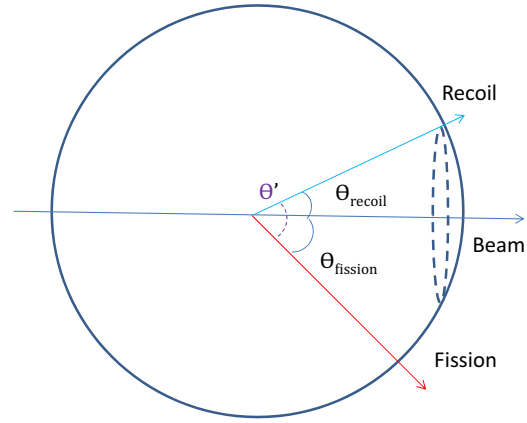

FIG. 12. Schematic diagram showing the angles of fission-fragment emission θ_{fission} and recoils θ_{recoil}. The dotted blue line represents possible out-of-plane recoil angles and θ' is the angle between the recoil direction and one of the fission fragments.

Averaging over the small circle on the figure corresponds to averaging over the angle Φ_{recoil} which selects the term $m = 0$ in the sum, and one ends up with the second Legendre polynomial when inserting into the angular distribution after averaging:

$$W(\theta_{\text{fission}}) = 1 + A_2 P_2(\cos\theta_{\text{recoil}}) P_2(\cos\theta_{\text{fission}}). \quad \text{(A2)}$$

Thus, one sees that this averaging over directions of the recoil restores the symmetry with respect to the beam axis. Thus, in the rest frame of recoil nucleus, the angular distribution coefficient with respect to the beam axis is related to the one of the in-plane distribution by just an extra factor $P_2(\cos\theta_{\text{recoil}})$.

[1] P. K. Rath, S. Santra, N. L. Singh, R. Tripathi, V. V. Parkar, B. K. Nayak, K. Mahata, R. Palit, S. Kumar, S. Mukherjee *et al.*, Phys. Rev. C **79**, 051601(R) (2009).

[2] C. S. Palshetkar, S. Santra, A. Chatterjee, K. Ramachandran, S. Thakur, S. K. Pandit, K. Mahata, A. Shrivastava, V. V. Parkar, and V. Nanal, Phys. Rev. C **82**, 044608 (2010).

[3] V. V. Parkar, R. Palit, S. K. Sharma, B. S. Naidu, S. Santra, P. K. Joshi, P. K. Rath, K. Mahata, K. Ramachandran, T. Trivedi *et al.*, Phys. Rev. C **82**, 054601 (2010).

[4] M. K. Pradhan, A. Mukherjee, P. Basu, A. Goswami, R. Kshetri, R. Palit, V. V. Parkar, M. Ray, S. Roy, P. R. Chowdhury *et al.*, Phys. Rev. C **83**, 064606 (2011).

[5] P. K. Rath, S. Santra, N. L. Singh, K. Mahata, R. Palit, B. K. Nayak, K. Ramachandran, V. V. Parkar, R. Tripathi, and S. K. Pandit, Nucl. Phys. A **874**, 14 (2012).

[6] P. K. Rath, S. Santra, N. L. Singh, B. K. Nayak, K. Mahata, R. Palit, K. Ramachandran, S. K. Pandit, A. Parihari, A. Pal *et al.*, Phys. Rev. C **88**, 044617 (2013).

[7] N. Keeley, S. J. Bennett, N. M. Clarke, B. R. Fulton, G. Tungate, P. V. Drumm, M. A. Nagarajan, and J. S. Lilley, Nucl. Phys. A **571**, 326 (1994).

[8] A. M. M. Maciel, P. R. S. Gomes, J. Lubian, R. M. Anjos, R. Cabezas, G. M. Santos, C. Muri, S. B. Moraes, R. L. Neto, N. Added *et al.*, Phys. Rev. C **59**, 2103 (1999).

[9] H. Kumawat, V. Jha, B. J. Roy, V. V. Parkar, S. Santra, V. Kumar, D. Dutta, P. Shukla, L. M. Pant, A. K. Mohanty *et al.*, Phys. Rev. C **78**, 044617 (2008).

[10] S. Santra, S. Kailas, K. Ramachandran, V. V. Parkar, V. Jha, B. J. Roy, and P. Shukla, Phys. Rev. C **83**, 034616 (2011).

[11] G. R. Kelly, N. J. Davis, R. P. Ward, B. R. Fulton, G. Tungate, N. Keeley, K. Rusek, E. E. Bartosz, P. D. Cathers, D. D. Caussyn *et al.*, Phys. Rev. C **63**, 024601 (2000).

[12] S. Santra, V. V. Parkar, K. Ramachandran, U. K. Pal, A. Shrivastava, B. J. Roy, B. K. Nayak, A. Chatterjee, R. K. Choudhury, and S. Kailas, Phys. Lett. B **677**, 139 (2009).

[13] H. Kumawat, V. Jha, B. J. Roy, V. V. Parkar, S. Santra, V. Kumar, D. Dutta, P. Shukla, L. M. Pant, A. K. Mohanty *et al.*, Phys. Rev. C **81**, 054601 (2010).
[14] S. Santra, S. Kailas, V. V. Parkar, K. Ramachandran, V. Jha, A. Chatterjee, P. K. Rath, and A. Parihari, Phys. Rev. C **85**, 014612 (2012).
[15] H. Freiesleben, f. G. T. Rizzo, and Z. R. Huizenga, Phys. Rev. C **12**, 42 (1975).
[16] I. Itkis, A. Bogacheva, A. Chizhov, D. Gorodisskiy, M. Itkis, G. Knyazheva, N. Kondratiev, E. Kozulin, L. Krupa, S. Mulgin *et al.*, Phys. Lett. B **640**, 23 (2006).
[17] A. Parihari, S. Santra, A. Pal, N. L. Singh, K. Mahata, B. K. Nayak, R. Tripathi, K. Ramachandran, P. K. Rath, R. Chakrabarti *et al.*, Phys. Rev. C **90**, 014603 (2014).
[18] S. Santra, A. Pal, P. K. Rath, B. K. Nayak, N. L. Singh, D. Chattopadhyay, B. R. Behera, V. Singh, A. Jhingan, P. Sugathan *et al.*, Phys. Rev. C **90**, 064620 (2014).
[19] J. Lestone, J. Leigh, J. Newton, and J. Wei, Nucl. Phys. A **509**, 178 (1990).
[20] S. Kailas, D. M. Nadkarni, A. Chatterjee, A. Saxena, S. S. Kapoor, D. Chattopadhyay, R. Vandenbosch, J. P. Lestone, J. F. Liang, D. J. Prindle *et al.*, Phys. Rev. C **59**, 2580 (1999).
[21] N. Majumdar, P. Bhattacharya, D. C. Biswas, R. K. Choudhury, D. M. Nadkarni, and A. Saxena, Phys. Rev. C **51**, 3109 (1995).
[22] D. J. Hinde, M. Dasgupta, J. R. Leigh, J. P. Lestone, J. C. Mein, C. R. Morton, J. O. Newton, and H. Timmers, Phys. Rev. Lett. **74**, 1295 (1995).
[23] H. Zhang, J. Xu, Z. Liu, J. Lu, K. Xu, and M. Ruan, Phys. Lett. B **218**, 133 (1989).
[24] P. Dyer, R. J. Puigh, R. Vandenbosch, T. D. Thomas, M. S. Zisman, and L. Nunnelley, Nucl. Phys. A **322**, 205 (1979).
[25] K. L. Wolf, R. Vandenbosch, and W. D. Loveland, Phys. Rev. **170**, 1059 (1968).
[26] G. R. Satchler, *Introduction to Nuclear Reactions* (Macmillan, New York, 1980).
[27] V. E. Viola, K. Kwiatkowski, and M. Walker, Phys. Rev. C **31**, 1550 (1985).
[28] J. Fernandez-Niello, C. H. Dasso, and S. Landowne, Comp. Phys. Commun. **54**, 409 (1989).
[29] B. K. Nayak, R. G. Thomas, R. K. Choudhury, A. Saxena, P. K. Sahu, S. S. Kapoor, R. Varma, and D. Umakanth, Phys. Rev. C **62**, 031601(R) (2000).
[30] A. J. Sierk, Phys. Rev. C **33**, 2039 (1986).
[31] NRV, http://nrv.jinr.ru/nrv/webnrv/fission/.
[32] V. S. Ramamurthy and S. S. Kapoor, Phys. Rev. Lett. **54**, 178 (1985).
[33] D. Vorkapic and B. Ivanisevic, Phys. Rev. C **52**, 1980 (1995).
[34] J. P. Lestone, A. A. Sonzogni, M. P. Kelly, and R. Vandenbosch, Phys. Rev. C **56**, R2907 (1997).
[35] R. G. Thomas, B. K. Nayak, A. Saxena, D. C. Biswas, L. M. Pant, and R. K. Choudhury, Phys. Rev. C **65**, 057601 (2002).
[36] A. N. Behkami, Nucl. Data. Tables **10**, 1 (1971).